

# RADIAL-SECTOR CYCLOTRONS WITH DIFFERENT HILL AND VALLEY FIELD PROFILES

M.K. Craddock<sup>#</sup>, University of British Columbia and TRIUMF\*, Vancouver, B.C., Canada

## Abstract

A new class of isochronous cyclotron is described in which more general radial field profiles  $B(r)$  are allowed than the simple proportionality to total energy found in conventional radial- and spiral-sector cyclotrons. Isochronism is maintained by using differently shaped field profiles in the hills and valleys. Suitably chosen profiles will produce high flutter factors and significant alternating-gradient focusing, enabling vertical focusing to be maintained up to 1 GeV or more using radial rather than spiral sectors.

## INTRODUCTION

In an isochronous cyclotron, the constant orbit frequency, independent of ion energy  $\gamma m_0 c^2$  and average radius  $R$  (circumference/ $2\pi$ ), implies that

$$B = \gamma B_c, \quad R = \beta R_c, \quad (1)$$

where  $B$  denotes the average field around a closed orbit,  $B_c$  the “central field” and  $R_c$  the “cyclotron radius”. Unfortunately the resultant positive field gradient produces a defocusing contribution to the vertical betatron tune  $\nu_z$  given by  $\Delta\nu_z^2 = -\beta^2\gamma^2$ . From the beginning, a major problem in cyclotron design has been how to compensate this and ensure vertical focusing. Thomas’s [1] suggestion of edge focusing through an azimuthal field variation with  $N$ -fold symmetry, and Kerst’s [2] of adding alternating focusing by using spiral sectors, have together succeeded in enabling “compact” cyclotrons with spiral sectors to accelerate protons to 230 MeV ( $\beta^2\gamma^2 = 0.55$ ) [3]. *Separate-sector cyclotrons* (SSCs) can achieve higher flutter and so higher energies: the PSI Ring Cyclotron [4] produces 590 MeV protons ( $\beta^2\gamma^2 = 1.65$ ), and designs have been published for energies, up to 15 GeV [5].

*Reverse-bend cyclotrons* would achieve higher flutter still by making the valley fields negative ( $B_v = -B_h$ , as in radial-sector FFAGs), rather than zero. Moreover, the alternating-gradient (AG) focusing, minimal in the previous schemes, becomes significant. Thus, if the hills cover a fraction of the orbit  $h = 0.6$ , the flutter is expected to maintain vertical focusing only up to 3.75 GeV. But a tracking simulation [6] has shown that positive focusing is in fact preserved up to 7.3 GeV.

## HILL AND VALLEY FIELD PROFILES

A common feature of the above schemes is that the hill and valley fields, while of different magnitudes, are assumed to have the same radial profiles, *i. e.*:

$$B_v(r)/B_h(r) = \text{constant} \quad (2)$$

More elaborate designs have also been proposed to achieve isochronism at high energy without using spiral magnets – basically by introducing more free parameters. Thus Rees [7] has designed a non-scaling muon FFAG that remains isochronous over the range 8-20 GeV ( $5,900 < \beta^2\gamma^2 < 37,000!$ ), relying on AG focusing by “pumpet” cells (OdoFoDoFodO) composed of five straight-sided magnets of three different designs. On a less ambitious scale, Johnstone [8, 9] has designed close-to-isochronous non-scaling proton FFAGs to provide 250-MeV protons and 400-MeV carbon ions for cancer therapy, and 1-GeV protons for ADSR. These all use a 4-cell FDF triplet lattice with straight-sided (though not necessarily radial) edges, and are also remarkable for their low variation in tune, both  $\nu_z$  and  $\nu_r$ . In both these authors’ studies the  $B(r)$  profile in each type of magnet is specially determined to produce the desired orbit properties.

Here we propose to explore a simpler possibility for achieving positive vertical focusing at high energy with purely radial sectors – allowing the radial field profiles in hills and valleys to differ. As was found helpful in previous high-energy cyclotron studies [6], we assume hard-edge fields with  $B_h$  and  $B_v$  each constant along equilibrium orbits. In particular we assume a polynomial variation with energy:

$$B_h(\gamma) = H_0 + H_1\gamma + H_2\gamma^2 + H_3\gamma^3 + \dots \quad (3)$$

$$B_v(\gamma) = V_0 + V_1\gamma + V_2\gamma^2 + V_3\gamma^3 + \dots \quad (4)$$

As a first step we consider a “compact” design with no drift spaces and negative valley fields. For an orbit of mean radius  $R$  crossing a hill-valley edge at radius  $R_e$ , we may write  $\ell_h = \rho_h\psi_h$  and  $\ell_v = \rho_v\psi_v$  for the arc lengths within a half-cell (Fig. 1), where the radii of curvature  $\rho_h = B_c R_c \beta \gamma / B_h(\gamma)$ ,  $\rho_v = B_c R_c \beta \gamma / B_v(\gamma)$ , and  $\psi_h$  and  $\psi_v$  are the bending angles.

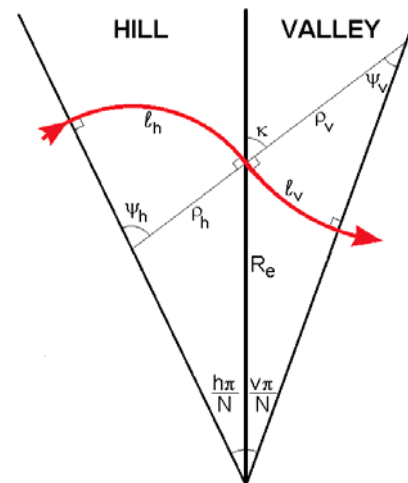


Figure 1: Orbit geometry within a half-cell.

\*TRIUMF receives federal funding under a contribution agreement through the National Research Council of Canada.

<sup>#</sup>craddock@triumf.ca

To maintain isochronism:

$$\ell_h H_1 + \ell_v V_1 = \frac{\pi}{N} B_c R_c \beta \quad \text{and} \quad \ell_h H_n + \ell_v V_n = 0 \quad (n \neq 1). \quad (5)$$

Thus if the hill coefficients  $H_n$  are specified, the valley coefficients  $V_n$  must satisfy:

$$V_1 = \frac{\pi}{N} \frac{B_c R_c}{\ell_v} \beta - \frac{\ell_h}{\ell_v} H_1 \quad \text{and} \quad V_n = -\frac{\ell_h}{\ell_v} H_n \quad (n \neq 1). \quad (6)$$

### Orbit Geometry

To compute  $B_v$  therefore requires knowledge of the bending angles  $\psi_h$  and  $\psi_v$  and of the radii of curvature – of which  $\rho_v$  itself depends on  $B_v$ . These parameters may be evaluated by invoking their various geometrical relationships, which after some manipulation yield a transcendental equation for  $\psi_h$ , from which the others follow:

$$\psi_h + (\psi_h - \pi/N) \frac{\sin \psi_h \sin[(1-h)\pi/N]}{\sin(\psi_h - \pi/N) \sin(h\pi/N)} = \frac{B_c \beta \gamma}{B_h(\gamma)}. \quad (7)$$

This must be solved numerically, but a good starting point is to make the approximation  $R_e = \beta R$ , giving:

$$\psi_{h0} = \arcsin\left(\frac{B_h(\gamma)}{\beta B_c} \sin\left(\frac{h\pi}{N}\right)\right). \quad (8)$$

### Betatron Tunes

To calculate the betatron tunes we take a lumped-element approach (validated by tracking with CYCLOPS in previous studies [6]), evaluating the traces of the vertical and horizontal transfer matrices for the full cell:

$$M = M_e M_v M_e M_h. \quad (9)$$

Here  $M_e$  is the standard  $2 \times 2$  matrix for a thin lens, while  $M_v$  and  $M_h$  are those for focusing and defocusing sector magnets respectively. For  $M_e$  we need to evaluate the focal power  $g$  of the edge crossing, which depends on the Thomas crossing angle  $\kappa = \psi_h - h\pi/N$  and is given by:

$$g = \frac{B_h - B_v}{B_c R_c \beta \gamma} \tan\left(\psi_h - \frac{h\pi}{N}\right). \quad (10)$$

For  $M_v$  and  $M_h$  we need the field gradients and the phase advances  $\phi_{h,v}$ . For vertical motion  $\phi_h = \ell_h \sqrt{K_h}$  and  $\phi_v = \ell_v \sqrt{K_v}$ , where the respective coefficients  $K_h$  and  $K_v$  are:

$$K_h = \frac{dB_h/dr}{B_c R_c \beta \gamma} = \frac{\gamma^2}{B_c R_c^2} (H_1 + 2H_2 \gamma + 3H_3 \gamma^2 + \dots), \quad (11)$$

$$K_v = \frac{dB_v/dr}{B_c R_c \beta \gamma} = \frac{\gamma^2}{B_c R_c^2} (V_1 + 2V_2 \gamma + 3V_3 \gamma^2 + \dots). \quad (12)$$

For the horizontal motion the phase advances are  $\phi_h^* = \ell_h \sqrt{K_h^*}$  and  $\phi_v^* = \ell_v \sqrt{K_v^*}$ , where:

$$K_h^* = \frac{1}{\rho_h^2} + K_h \quad \text{and} \quad K_v^* = \frac{1}{\rho_v^2} - K_v. \quad (13)$$

## RESULTS

A number of cases were studied with  $H_0 = 0 = H_{n>2}$  to investigate the dependence of the tunes on the size of the  $H_1$  and  $H_2$  components, the hill fraction  $h$  and the number of sectors  $N$ . Most runs were made for  $h = 0.5$  and  $N = 8$ .

Figure 2 displays an example of such field profiles for one of the cases studied, showing that for  $H_2 = 0.2H_1$  the  $B_h$  required is 20-40% higher than in an SSC.

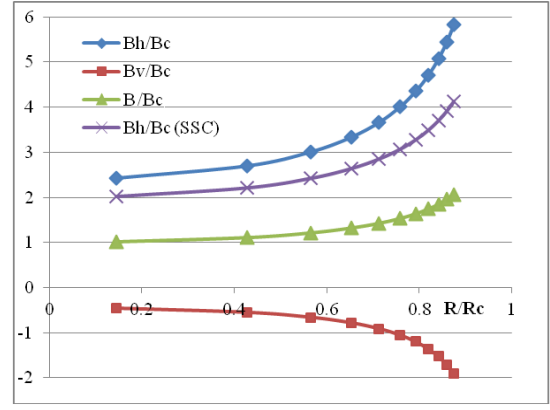


Figure 2: Field profiles for  $N = 8$ ,  $h = 0.5$ ,  $H_1 = 2B_c$ ,  $H_2 = 0.4B_c$ .

For reference Fig. 3 displays the tunes for the conventional situation where  $H_2 = 0$  so that both  $B_h$  and  $B_v$  are directly proportional to  $\gamma$ . Results are shown for values of  $H_1/B_c$  between 2.0 and 2.6, the lower value representing the situation in a separated-sector cyclotron with  $h = 0.5$  and near-zero field in the valleys. In that case the flutter  $F^2 \approx 1$ , and as expected the vertical tune  $\nu_z$  drops towards zero as  $\beta^2 \gamma^2$  approaches 1 at around 400 MeV. Higher values of  $H_1/B_c$  require more negative valley fields, raising the flutter and the vertical tune values, until with  $H_1/B_c = 2.6$  positive focusing is retained up to 1 GeV. The effect of increased  $H_1/B_c$  on the horizontal tune is less dramatic: for  $H_1/B_c = 2$ ,  $\nu_r \approx \gamma$ , and for  $H_1/B_c = 2.6$   $\nu_r$  still grows linearly but ~40% faster.

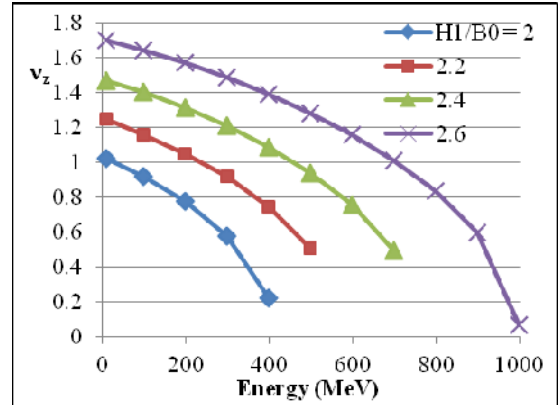


Figure 3: Variation of the vertical tune  $\nu_z$  with energy for  $H_2 = 0$ ,  $h = 0.5$ ,  $N = 8$ , and various values of  $H_1/B_c$ .

Figure 4 shows the effect of adding a  $\gamma^2$  component to the field for  $H_1/B_c = 2.0$ ,  $h = 0.5$  and  $N = 8$ . For  $H_2 = 0$  we have the same case as before, where the vertical tune drops to 0 near 400 MeV. But increasing the  $\gamma^2$  component raises  $\nu_z$  significantly, making it almost constant for  $H_2/B_c = 0.4$  and rise with energy for higher values. There is also a significant effect on the horizontal tune, introducing a noticeable quadratic dependence on energy, driving  $\nu_r$  to the  $N/2$  resonance at 900 MeV for  $H_2/B_c = 0.6$ .

In Fig. 5 we return to the effect of varying  $H_1/B_c$  (as in Fig. 2) for  $h = 0.5$  and  $N = 8$ , but now with  $H_2/B_c = 0.4$ . As before, raising  $H_1/B_c$  increases both tunes, but  $\nu_z$  more

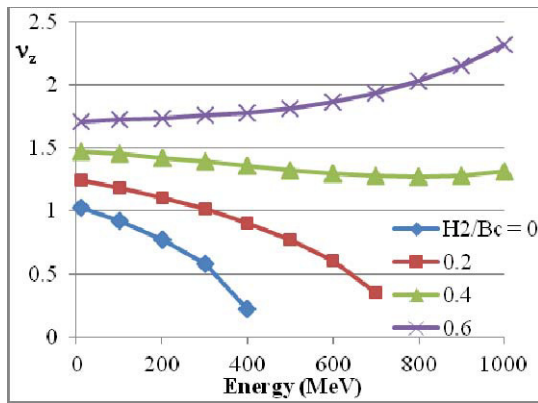


Figure 4: Variation of the vertical tune  $\nu_z$  with energy for  $H_1/B_c = 2$ ,  $h = 0.5$ ,  $N = 8$ , and various values of  $H_2/B_c$ .

noticeably than  $\nu_r$ . For this value of the  $\gamma^2$  component, the least variation in  $\nu_z$  is obtained for  $H_1/B_c = 2.2$ . In this case (and in those of varying  $h$  and  $N$  below) the effect on the horizontal tune is small.

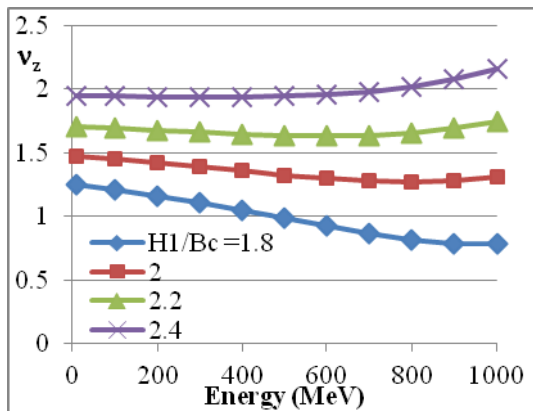


Figure 5: Variation of the vertical tune  $\nu_z$  with energy for  $H_2/B_c = 0.4$ ,  $h = 0.5$ ,  $N = 8$ , and various values of  $H_1/B_c$ .

The fraction of a sector occupied by the hill also has a powerful influence on the tunes. Figure 6 shows the tunes for hill fractions  $h$  between 0.5 and 0.65 for  $H_1/B_c = 2$ ,  $H_2/B_c = 0.4$  and  $N = 8$ . Just as for separated-sector cyclotrons, widening the hills increases the flutter and both  $\nu_z$  and  $\nu_r$ .

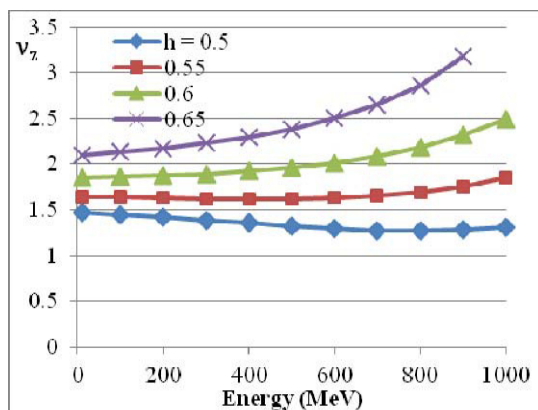


Figure 6: Variation of the vertical tune  $\nu_z$  with energy for  $H_1/B_c = 2$ ,  $H_2/B_c = 0.4$ ,  $N = 8$ , and various values of  $h$ .

The effect of the number of sectors on the tunes is shown in Fig. 7, where data are plotted for  $N = 8, 10$  and  $12$ , with  $H_1/B_c = 2$ ,  $H_2/B_c = 0.4$  and  $h = 0.5$ . Increasing  $N$  lowers both  $\nu_z$  and  $\nu_r$ , but the effect is a weak one except at the highest energies. Neither tune approaches the  $N/2$  resonance in the energy range considered, but  $\nu_r$  would do so for  $N = 8$  not much above 1 GeV, making higher periodicity necessary for higher-energy designs.

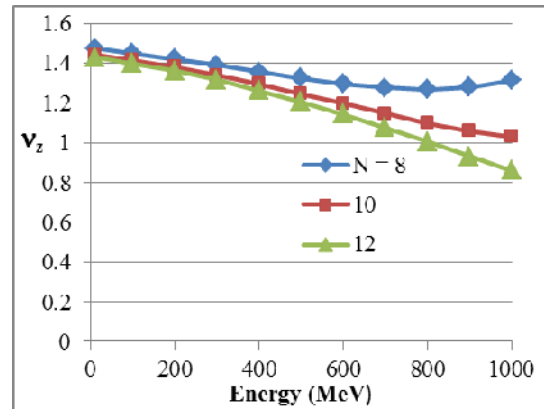


Figure 7: Variation of the vertical tune  $\nu_z$  with energy for  $H_1/B_c = 2$ ,  $H_2/B_c = 0.4$ ,  $h = 0.5$ , and various values of  $N$ .

## CONCLUSIONS

A study has begun of using different radial field profiles in hills and valleys (while maintaining isochronism) to obtain increased flutter and more strongly alternating gradients – and hence increased vertical focusing – in radial-sector cyclotrons. As a first step, adding a  $\gamma^2$  component to the hill fields in a “compact” design (i.e. no field-free regions) – and subtracting a compensating  $\gamma^2$  component from the valley fields – has been shown to be a possible way of providing radial-sector cyclotrons with sufficient vertical focusing to reach at least 1 GeV.

The practicality of such a design has not been taken into account, particularly with regard to finding suitable locations for the accelerating cavities and injection and extraction systems. Field-free drift spaces would remove this difficulty and a beam optics study of such an arrangement is under way.

## REFERENCES

- [1] L.H. Thomas, *Phys. Rev.* **54**, 580-8 (1938).
- [2] D.W. Kerst, *et al.*, *Phys. Rev.* **98**, 1153 (A) (1955).
- [3] Y. Jongen *et al.*, *Proc. PAC'97*, 3816 (IEEE, 1998).
- [4] H. Willax, *Proc. Int. Conf. Sector-focused Cyclotrons & Meson Factories*, CERN 63-19, 386-97 (1963).
- [5] J.I.M. Botman, M.K. Craddock, *et al.*, *Proc. PAC'83*, *IEEE Trans.* **NS-30**, 2007-9 (1983).
- [6] M.K. Craddock, Y.-N. Rao, *PAC'09*, 5044 (2009).
- [7] G. Rees, *ICFA Beam Dynamics Newsltr.* **43**, 74 (2007).
- [8] C. Johnstone, *FFAG'09* (2009).
- [9] C. Johnstone, P. Snopok, F. Méot, W. Weng, *Proc. IPAC'12*, 4118 (2012).